

PROXIMITY EFFECTS OF PIEZOELECTRIC ENERGY HARVESTERS IN FLUID FLOW

A. Deivasigamani*, **J.M. McCarthy***, **S.J. John***, **S. Watkins***, **F. Coman****
***School of Aerospace, Manufacturing, Mechanical Engineering, RMIT University, Melbourne, Australia, **FCST Pty. Ltd., P.O.Box No. 122, Melbourne, Australia.**

Keywords: *Energy Harvesting, Wind-induced Flutter, Proximity Effects, Phase Lag*

Abstract

Energy harvesting from wind was investigated using piezoelectric materials. Proximity effects of two harvesters were examined by displacing one with respect to another in the three orthogonal directions. Results indicated that in the stream-wise direction, the downstream harvester provided 20-40% more power output compared to the upstream one while the harvesters displaced in lateral and vertical directions did not exhibit any beneficial interactions. Simultaneous voltage measurements indicated that there existed a specific phase lag between the harvesters at a given wind speed, and that the phase lag had a non-linear relationship with the free-stream wind speed. The results and limitations are discussed in detail.

1 Introduction

Flutter of a flag, vibrations of antenna on the roof of a car and flutter of leaves on a tree appear to be very trivial day-to-day activities. However, they are complex engineering problems for researchers and scientists. Flow-induced flutter has been an area of study for a very long time. Work done in [1]-[3] have examined the theoretical phenomena of flutter of immersed solids with both finite and infinite dimensions, while in [4] this work was applied to the problem of aircraft wing flutter, and in [5], thin plates. In [6], vortex shedding characteristics were theoretically examined at the trailing edge of a fluttering plate with semi-infinite dimensions. In [7], a theoretical

analysis using linear-beam theory was used to determine the cause and mitigation of palatal flutter. In [7]-[9] the critical flutter speed (the flow speed at which the immersed beam begins to flutter) and flutter frequency characteristics of immersed beams in parallel flows were examined.

However, only recently, there has been a realization that flutter could be exploited for the purposes of energy harvesting, using highly compliant piezoelectric materials immersed in a fluid flow. Flutter is related to resonance of the system, and the amplitudes, and hence the strains induced in an object during flutter become large. In order to extract significant amounts of energy from a piezoelectric material, large mechanical strain must be applied. If this could be induced by flutter then energy can be extracted from a fluid flow.

One of the earliest attempts to realize this concept was in [10]; where flutter of a thin, Polyvinylidene-fluoride (PVDF) membrane was induced by introducing an upstream vortex-shedding, bluff body. The vortices would impinge on the flexible membrane, and due to the imposed pressure gradients, would cause time-varying membrane deformation according to the vortex shedding frequency of the bluff body. This method of flutter excitation was classed by [11] as Extraneously Induced Excitation (EIE) where flutter is induced from external pressure gradients caused by turbulence or vortices. In [12] a similar study was carried out, whereby a bluff body was used to excite undulations of the piezoelectric “eel” within a water flow. However, they focused their attention more on optimizing the electrical subsystem. Furthermore, in [13] two designs were suggested that could exploit vortex

shedding in a water flow; along with a simplified analysis, it was found that such a piezoelectric system, when scaled up, could have a higher power density than that of a conventional wind turbine. However, their calculations did not account for the distances between two consecutive harvesters in any direction.

In [14], a novel concept of a piezoelectric flutter system, that would not only be efficient, but aesthetically-pleasing and safe, was envisioned. A tree-like construct with multiple piezoelectric “stalks” with polymeric “leaves” attached the stalks formed the basis of this concept. Figure 1 shows this concept.

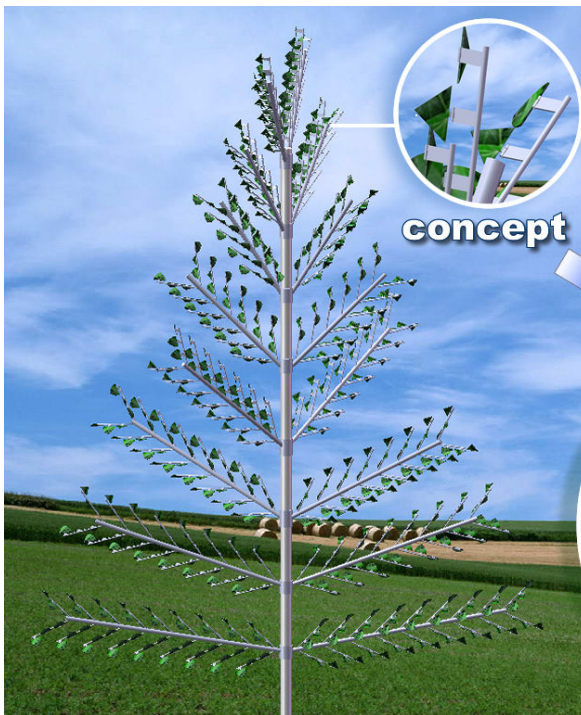


Fig. 1. The piezoelectric “tree” concept proposed in [14].

Work in [15] initiated research on this concept, by starting with a single piezoelectric, cantilevered leaf and stalk system in parallel, smooth flow. There was no vortex-shedding bluff body in this study, as flutter in this type of arrangement is meant to be self-induced. This type of flutter excitation was classified in [11] as Movement Induced Excitation (MIE). Here, flutter is caused by a small perturbation of the membrane in the flow and further growth of this instability. The harvester design in this

paper is similar to the design in the work reported here.

In [16], a similar harvester was investigated for its power output. Later, two such harvesters were placed along the direction of wind and the distance between them was varied. It was observed that at a specific distance, the downstream harvester produced higher power output compared to the downstream one. Recently, in [17], smoke flow visualization was performed to understand the flow structure downstream to the fluttering harvester to understand the interaction between the upstream and downstream harvester. However, the reasons for increased downstream power output were not fully understood. It is also important to note that the two harvesters, when placed together in lateral and vertical directions, did not have any change in the power output.

In this work, a harvester consisting of a PVDF stalk and a triangular polymeric leaf coupled with a hinge was examined. Two such harvesters, immersed in a smooth flow in three orthogonal directions (longitudinal, lateral and vertical directions) were investigated, one at a time, and the distances between them were varied. The power outputs of the harvesters were measured and these power outputs were compared with their stand-alone power outputs. Also, the time varying voltages from the PVDF's were recorded simultaneously to calculate the phase lag between the harvesters. The experimental method, setup and results are explained in the following sections.

2 Experimental setup

As discussed in the previous section, the aim of this work was to identify the influence of one harvester on the other, when two such harvesters were tested in three different orthogonal directions, one at a time. In the following sections, the wind-tunnel setup, experimental procedure, harvester configuration and data measurement are explained.

2.1 Wind-tunnel setup

The wind tunnel utilized in the experiments is a subsonic, closed-circuit design with an octagonal test section, measuring 1320mm high by 1070mm wide. A honeycomb mesh and an anti-turbulence screen, plus a 4:1 contraction ratio condition the incoming airflow, and give longitudinal turbulence intensity values of less than 0.3%. A 134-horsepower DC motor powers a six-bladed fan, permitting a maximum tunnel flow speed of approximately 45m/s. A pitotstatic tube linked to an MKS Baratron[®] was used for dynamic flow measurements, with flow speed being calculated using an air standard density value of 1.23kg/m³. A simple error analysis was carried out, in order to determine the impact of assuming a constant density across a large range of tests, and a maximum error of 0.5% in velocity measurements was obtained. Tunnel blockage due to the experimental setup was also found to be negligible.

2.2 Harvester configuration

Due to their flexibility, durability and relatively low cost, PVDF piezoelectric patches were utilized (Measurement Specialties, Inc., LDT1-028K/L type). The length, width and thickness of the piezoelectric patch were 72mm, 16mm and 205 μ m respectively. These patches were the same ones used in [15]. The work in [16] utilized Lead-Titanium-Zirconate (PZT) patches bonded to their steel beams; PZT being capable of outputting higher power than PVDF, but being generally less durable.

The leaves used for the experiments were fabricated from 0.35mm-thick polypropylene. Polypropylene was chosen due to its better fluttering characteristics which were evident from the work done in [18]. The shape of the leaf was an isosceles triangle with dimensions of 80mm by 80mm (base by height), as this was the shape and area that caused the PVDF's to output the highest power in previous work [19]. The leaf and piezoelectric stalk were coupled with a plastic revoluted hinge, which would allow free rotation of leaf about the vertical axis. Work done in [20] explained the

effect of a hinge in a fluttering cantilever system. The mass of the hinge was around 14% of the harvester mass, and was found to lower the fundamental flutter frequency by 30%, see [19]. The leading edge of the piezoelectric stalk was securely clamped and the leaf end was free. The clamping strip utilized for these experiments was 12mm wide. This length was chosen in order to securely hold the leads and wires attached to the PVDF stalk. The clamping strips were bolted to the wind-tunnel floor and ceiling, and guyed to the sidewalls to prevent any transverse oscillations. The clamping base was also taped, so as to prevent the piezoelectric electrodes from contacting the metal. The overall length (L) of the system with the piezoelectric stalk, leaf, hinge and the clamping strip were measured to be 180mm.

2.3 Experimental procedure

As mentioned earlier, two harvesters were placed in the following directions, one at a time:

1. Longitudinal/stream-wise direction.
2. Lateral/cross-stream direction.
3. Vertical direction.

In each direction, the separation distance (d) between the harvesters was varied. This distance is normalized with respect to the single leaf-stalk length (L) and expressed as (d/L). At first, the two harvesters were positioned at a normalized separation distance (d/L) of 0. Then, the separation distance was increased to 1 and 2. In the lateral direction, for the $d/L=0$ case, the separation distance was 10mm. This was because practically the harvesters should not be in physical contact with each other. However, for the other cases, the separation distances were maintained as explained above. Figures 2a, 2b and 2c show the schematic setup of the harvesters in stream-wise, vertical and cross-stream directions respectively. Figures 3a, 3b and 3c show the experimental setup of the harvesters in stream-wise, cross-stream and vertical directions respectively.

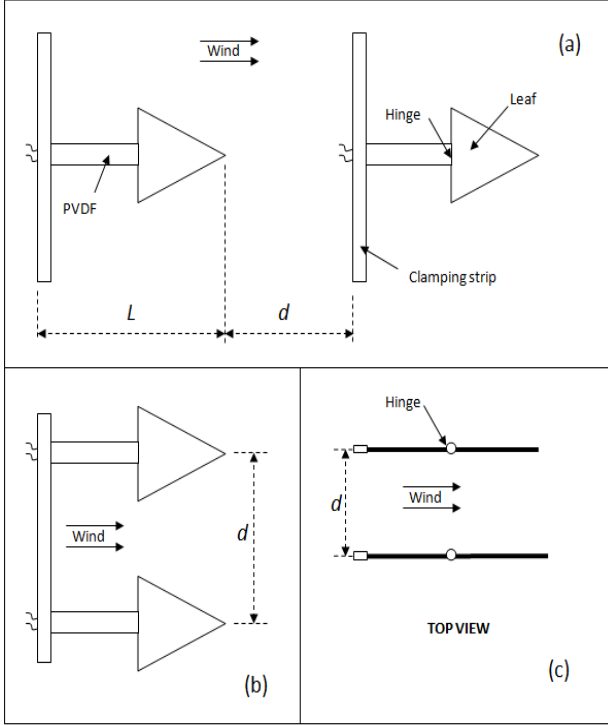


Fig. 2. Schematic of the harvesters in (a) stream-wise, (b) vertical and (c) cross-stream directions.

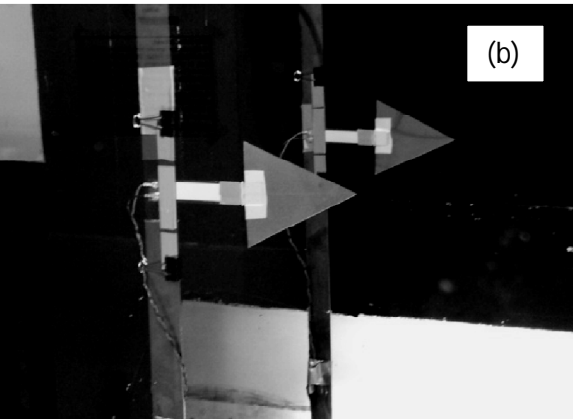
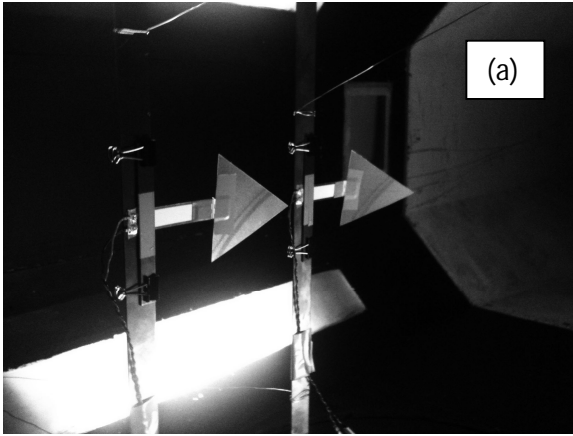


Fig. 3. Experimental setup of the harvesters in (a) stream-wise, (b) cross-stream and (c) vertical directions.

2.4 Electrical setup and data measurement

The piezoelectric stalks were connected to a simple parallel electrical circuit. The load resistance used for this experiment was $5.6\text{M}\Omega$. This value was experimentally obtained by recording the power output from a single leaf-stalk system across various load resistances in parallel (R_L); from $1.0\text{M}\Omega$ to $60\text{M}\Omega$, at a constant wind speed of 5.0m/s . This wind speed was chosen as the optimal speed since the tests were performed from 3m/s to 8m/s . These wind speeds aligned with the experiments performed in [15]. The voltages from the piezoelectric stalks were measured using a differential probe (Elditest, GE8115) which had a high internal resistance ($60\text{M}\Omega$) compared to the load resistance. The data from the differential probe was sent to a DAQ board (National Instruments, BNC2110) and the RMS voltage (V_{RMS}) of the AC waveform was calculated in 0.1 -second intervals using LabView[®]. The electrical power generated in 0.1s of leaf-stalk flutter is given by Eqn. 1:

$$P_i = \frac{V_{RMS_i}^2}{R_L} \quad (1)$$

Then, the total average power generated over the 30 -second data acquisition window was calculated as:

$$P_{ave} = \frac{1}{300} \sum_{i=1}^{300} P_i \quad (2)$$

These wind speeds aligned with the experiments performed in [15]. Figure 4 shows the circuit employed in the experiments.

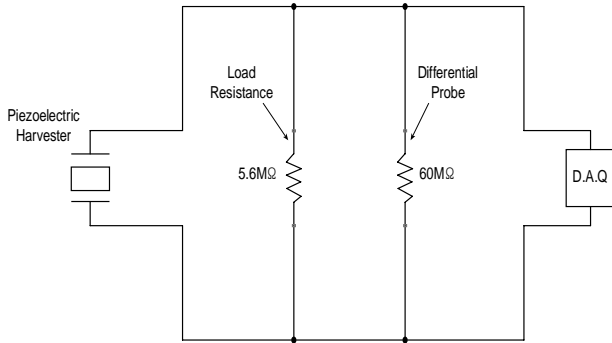


Fig. 4. Parallel circuit used to measure power from the harvesters.

3 Results and discussion

In order to understand the proximity effects of the harvesters, it was first important to look at how the harvester performed when it stood alone in the wind tunnel. Figure 5 shows the power output of a single harvester when immersed in parallel fluid flow from 3m/s to 8m/s.

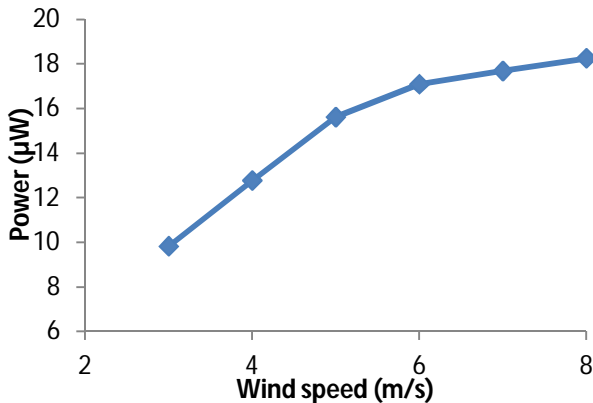


Fig. 5. Power output of a stand-alone harvester.

From figure 4, it is evident that as the wind speed is increased, the power output also increased. This phenomenon is due to the fact that as the wind speed increased, the amplitude and frequency of flutter increased which in turn increased the rate of change of strain on the PVDF. A maximum power of 18.3μW was recorded at 8m/s. The experiments (also in the

future sections) were performed twice and it was found that they were very repeatable.

In the following sections, stream-wise, cross-stream and vertical proximity effect results are explained. In order to compare the power output of a single harvester placed in tandem with its stand alone power output, a non-dimensionalized power output (λ) is defined as:

$$\lambda = \frac{P_{\text{actual}}}{P_{\text{stand-alone}}} \quad (3)$$

Thus, in the following sections, λ is used to estimate the effect of one harvester on the other. For example, a λ value of 1.10 would mean that the harvester outputs 10% more power when placed in tandem compared to its stand-alone power output.

3.1 Stream-wise proximity

As mentioned earlier, two harvesters were placed along the direction of the wind and the separation distance between them was varied (refer figure 2a). Figure 6 indicates the value of λ at all the wind speeds tested for the upstream harvester.

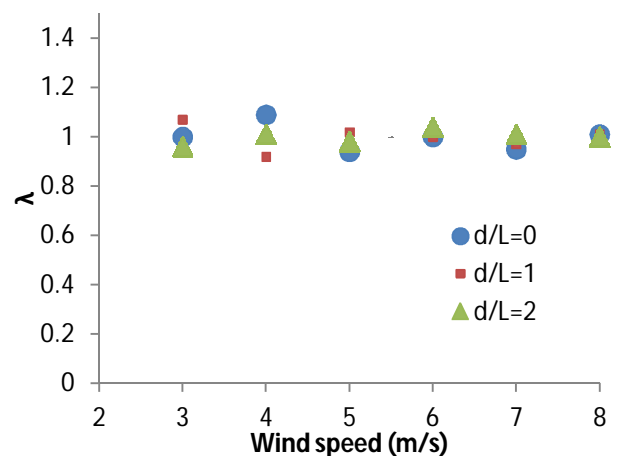


Fig. 6. Non-dimensionalized power output of the upstream harvester in longitudinal proximity tests.

Figure 6 indicates that the λ value remained close to 1 during different separation distances at all wind speeds for the upstream harvester.

This meant that the upstream harvester was not affected by the downstream harvester, when the downstream harvester's distance from the upstream one was varied. It is also important to mention that at lower wind speeds, the variation of power was more, which reflected in the higher variation of λ at 3m/s and 4m/s (+/- 8%).

However, it was interesting to observe the non-dimensionalized power output of the downstream harvester when the separation distance was varied. Figure 7 indicates the non-dimensionalized power output of the downstream harvester fluttering in tandem. The figure indicates that for all the separation distances, the λ value was found to be greater than 1 with a maximum value of 1.41 at a wind speed of 8m/s for all separation distances. The graph reveals that for a separation distance of $d/L=1$, the downstream harvester provided more power output compared to the other separation distances. The results indicated that the downstream harvester provided more power output when operated in tandem with an upstream harvester compared to its stand-alone operation. Also, there existed a specific distance ($d/L=1$ in this case) between the upstream and downstream harvesters, where the power output of the downstream harvester remained higher compared to the other separation distances. That said, it is important to note that this specific distance could be different if the dimensions and physical properties of the harvesters were varied. The results are explained later in the paper.

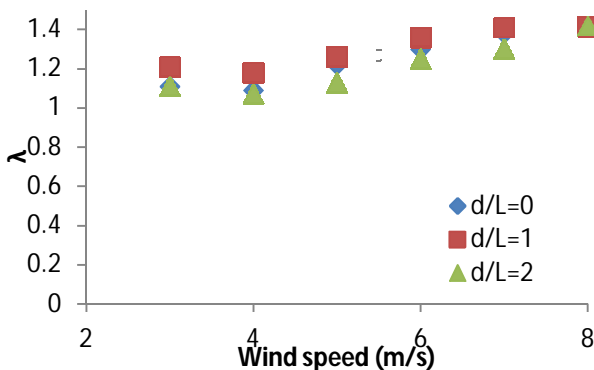


Fig. 7. Non-dimensionalized power output of the downstream harvester.

3.2 Cross-stream proximity

In these tests, two similar harvesters were placed laterally (side by side) and the separation distance between them were kept at $d/L=0, 1$ and 2 . Figures 8 and 9 show the non-dimensionalized power output of the 'left' and 'right' harvesters when operating in tandem at different separation distances.

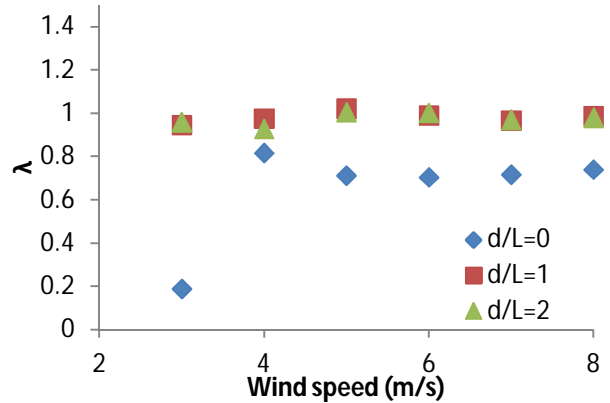


Fig. 8. Non-dimensionalized power output of the 'left' harvester in lateral proximity tests.

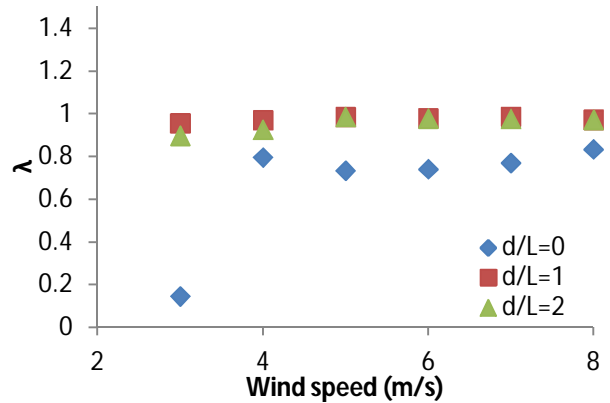


Fig. 9. Non-dimensionalized power output of the 'right' harvester in lateral proximity tests.

Figures 8 and 9 indicate that the behavior of left and right harvesters were similar. This result was expected as the configuration was symmetrical (the harvesters were placed side by side). At a lateral separation distance of 10mm ($d/L=0$), it was observed that the power output of the harvesters dropped significantly compared to their stand-alone case. Importantly, for $d/L=0$, at 3m/s, it was observed that the harvester provided only 18% of their stand-alone power output. It is proposed that at

this separation distance, the system had different fluid boundary conditions and hence behaved like a single bimorph unit and hence had a reduction in the effective compliance thereby reducing the power output. This indicated that at a small separation distance, the harvesters destructively interacted with each other unlike the longitudinal proximity case where the interaction was constructive. However, at separation distances of 180mm and 360mm ($d/L=1$ and 2), there was not much interaction and the harvesters fluttered independent of each other. This was reflected in the λ values (approximately 1) at these distances for all wind speeds.

3.3 Vertical proximity

In vertical proximity, two of the similar harvesters were placed vertically (one below the other) and their interaction with each other was observed in a similar manner to the cross-stream proximity experiments. Figures 10 and 11 show the non-dimensionalized power output of the 'top' and 'bottom' harvester.

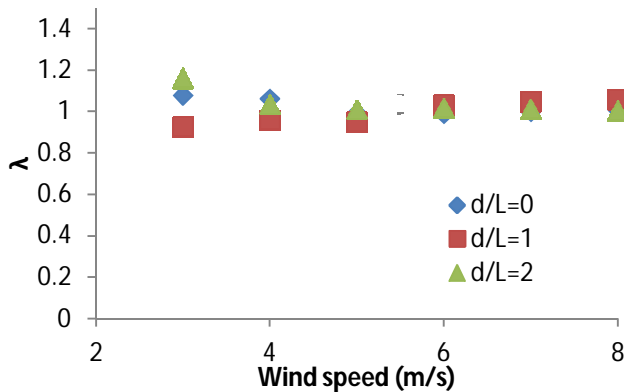


Fig. 10. Non-dimensionalized power output of the 'top' harvester in vertical proximity tests.

From the figures 10 and 11, it is evident that the λ values remained close to one for all the test cases except at a wind speed of 3m/s where there was a small variation in the λ value (+/- 8%). This behavior was also observed in the upstream harvester in the longitudinal case. As mentioned earlier, this could be due to the fact that at lower wind speeds, the harvesters did not achieve a uniform harmonic flutter compared to their flutter at higher wind speeds.

Also, at lower wind speeds, the flow in the wind tunnel could have been slightly more turbulent compared to the flow at higher wind speeds leading to a higher variation of λ values. However, it is evident that in the vertical proximity tests, there is no noticeable interaction between the two harvesters. The harvesters were found to be independent of each other in the vertical direction.

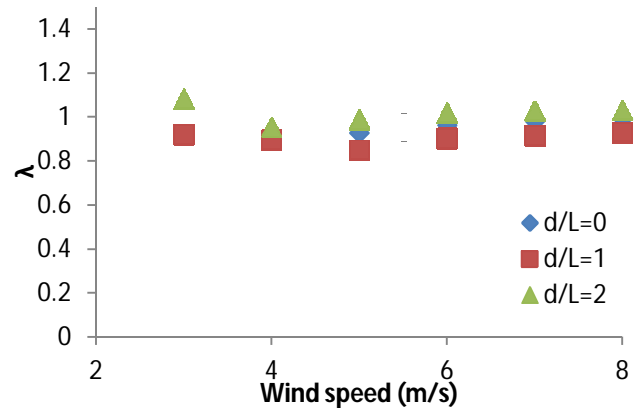


Fig. 11. Non-dimensionalized power output of the 'bottom' harvester in vertical proximity tests.

From the above sections, within the scope of the experiments, it was evident that only the stream-wise separation distance proved to have a beneficial interaction, thereby increasing the power output of the downstream harvester. Thus, in the following section, simultaneous voltage measurements were carried out to estimate the phase lag between the harvesters displaced in longitudinal direction only.

3.4 Simultaneous Voltage measurements

It was important to first understand the aerodynamic interaction between the harvesters. For this purpose, the authors conducted a smoke wire flow visualization to observe the downstream flow structure of the harvesters operating in tandem. Figure 12 shows an image of the flow visualization performed. The details are not provided here but the interested reader may find the results in [21]. From the images it was evident that there existed a phase lag between the upstream and downstream harvesters and it was proposed that

the vortex shed from the upstream harvester reached the downstream harvester at a critical position and constructively interacted with the downstream piezo such that the power output was elevated.

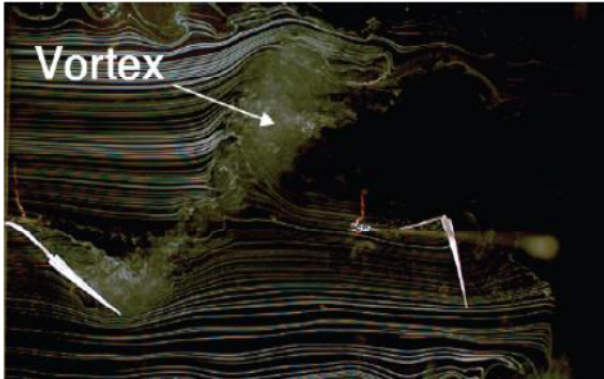


Fig. 12. Smoke wire flow visualization indicating the vortex shed by the upstream harvester.

Time varying voltage data of both the harvesters were recorded simultaneously using the LabView® interface using two identical circuits as shown in figure 4. These voltage data were then overlapped and based on their cycle timings, the phase lag was calculated at every wind speed. Also, two different load resistances (5.6MΩ and 3.4MΩ) were used to identify the influence of load matching on the phase lag. Table 1 shows the phase lag at different wind speeds between the harvesters.

Table 1. Phase lag between two harvesters in stream-wise direction at two different load resistances.

Wind speed (m/s)	Phase lag (deg.)	
	@ 5.6MΩ Load resistance	@3.4MΩ Load resistance
3	5.9	9.2
4	46.1	42.6
5	-	-
6	-	-
7	51.4	48.4
8	71.5	67.6

From the above table, it is clearly evident that the phase lags are different at different wind speeds. At 3m/s, it is seen that the phase lags are slightly different for both cases. However, it was also observed that the standard deviations

were quite high. Also, at wind speeds of 4, 7 and 8 m/s, it is clearly seen that there is not much variation in the phase lags. This proves that there is no significant effect of the electrical circuit on the phase relationship between the upstream and downstream piezos. Also, it indicates that the phase relationship is fairly repeatable and consistent at these wind speeds. In fact, each test was performed twice and the average phase lag was found to be the same. Figure 13 shows the phase lag at 4 m/s between the upstream and downstream piezo over the number of cycles recorded.

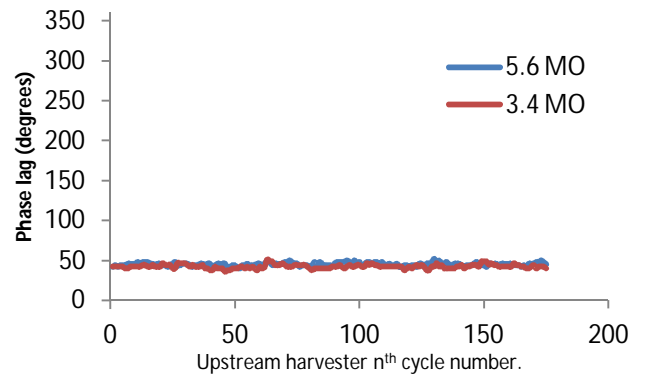


Fig. 13. Phase lag between the harvesters at 4m/s.

However, at 5 and 6 m/s, it was observed that there was not a constant phase lock between the upstream and downstream piezo. The phase lag varied from 0 to 360 degrees over time. Figure 14 shows the variation of phase lag for the number of cycles recorded at 6 m/s.

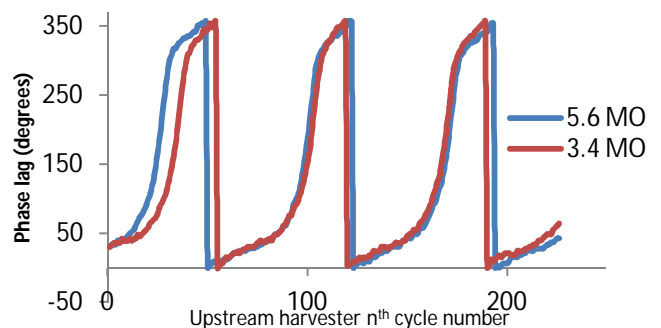


Fig. 14. Phase lag between the harvesters at 6m/s.

The above graph shows that there is no constant phase lock between the upstream and downstream piezo-leaf system. However, the

data also indicates that the behaviour of the phase lag is steady state. In order to understand this behaviour, the frequencies of the harvesters at this wind speed were investigated. Figure 15 shows the frequencies of flutter of the harvesters over the recorded number of cycles at 6m/s. The frequencies were calculated based on each cycle time and hence has a coarse resolution. However, that did not affect the findings of this analysis.

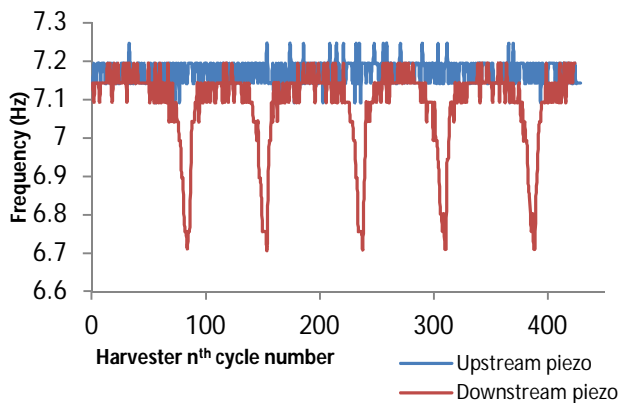


Fig. 15. Frequencies of the harvesters at 6m/s.

It can be seen that the frequency of the downstream harvester drops at regular intervals at this wind speed, and at the rest of the time, remains closer to the frequency of the upstream harvester. This indicates that the downstream harvester slows down at regular intervals creating a phase lag to vary from 0^0 to 360^0 . Also it was also observed that the amplitude of flutter of the downstream piezo remained larger compared to the upstream piezo throughout the test run resulting in a higher power output.

Thus, the vortices shed from the upstream harvester, when impinging on the downstream harvester, can have a constructive or a destructive impact on the power output. At a separation distance of one harvester length, it was observed that there was clearly a more constructive impact compared to other separation distances. Also at 5m/s and 6m/s, for this particular separation distance, it is believed that there was a destructive impact at regular intervals due to the vortices shed from the harvester upstream. However, the reason for the existence of a specific phase lag at every wind speed is still unclear and investigating it will form a part of the future work.

4 Conclusions

To conclude, two piezoelectric energy harvesters were placed in parallel smooth wind flow in three orthogonal directions, one direction at a time, and the separation distance between the harvesters were varied. Results indicated that when the harvesters were placed along the direction of the wind (longitudinal), the downstream harvester provided 20-40% more power output compared to its stand-alone case, especially at a separation distance of $d/L=1$. Also, when the harvesters were placed cross-stream with a very small separation distance (10mm), the harvesters produced only 20% of their stand-alone power indicating that they destructively interacted with each other. In all the other directions and separation distances, the harvesters' operation seemed to be independent of each other.

Simultaneous voltage measurements revealed that, in the stream-wise direction, there existed a specific phase lag between the harvesters at every wind speed and the phase lag and wind speed did not have any linear relationship. It is believed that the vortex shed from the upstream harvester has a constructive impact on the power output of the downstream harvester. Also, at certain wind speeds, the upstream vortex regularly disturbed the flutter of the downstream harvester. The reason for a specific phase lag between the harvesters in tandem is still to be understood in full. However, it is clear that when these piezoelectric harvesters are scaled up for energy generation, they could be intelligently placed in space to increase the overall power output from these energy harvesters.

The experiments performed involved only two harvesters operating at a given time in orthogonal directions. The interaction of multiple harvesters with each other, especially when displaced in stream-wise direction, is still to be investigated and will form a part of the future work.

Acknowledgments

This work was funded under Australian Research Council (ARC) Linkage grant

LP100200034 in conjunction with the Partner Organisation - Fabrics & Composites Science & Technology (FCST) Pty Ltd.

References

- [1] Paidoussis, M., *Fluid-Structure Interactions- Slender Structures and Axial Flow*, Elsevier Academic Press, Vol. 1, 1998.
- [2] Paidoussis, M., Price, S.J. and de Langre, E., *Fluid-Structure Interactions - Cross Flow-Induced Instabilities*, Cambridge University Press, 2011.
- [3] Lord Rayleigh, *Proc. Lond. Math. Soc.*, Vol. X, pp. 4-13, 1879.
- [4] Theodorsen, T. *General Theory of Aerodynamic Instability and the Mechanism of Flutter*. NACA Tech. Rep. No. 496, 1935.
- [5] Kornecki, A., Dowell, E.H. and O'Brien, J. On the aerodynamic instability of two dimensional panels in uniform incompressible flow. *Journal of Sound and Vibration*, Vol. 47, No. 2, pp. 163-178, 1976.
- [6] Frederiks, W., Hilberink, H.C.J. and Sparenberg, J.A. On the Kutta condition for the flow along a semi-infinite elastic plate. *Journal of Engineering Mathematics*, Vol. 20, pp. 27-50, 1986.
- [7] Huang, L. Flutter of Cantilevered Plates in Axial Flow. *Journal of Fluids and Structures*, Vol. 9, pp. 127-147, 1995.
- [8] Zhang, J., Childress, S., Libchaber, A. and Shelley, M. Flexible filaments in a flowing soap film as a model for one-dimensional flags in a two-dimensional wind. *Nature*, Vol. 408, pp. 835-839, 2000.
- [9] Argentina, M. and Mahadevan, L. Fluid-flow-induced flutter of a flag. *Proceedings of the National Academy of Sciences of the United States of America*, Vol. 102, No. 6, pp. 1829-1834, 2005.
- [10] Allen, J.J. and Smits, A.J. Energy Harvesting Eel. *Journal of Fluids and Structures*, Vol. 15, No. 3-4, pp. 629-640, 2001.
- [11] Naudascher, E. and Rockwell, D. Oscillator-model approach to the identification and assessment of flow-induced vibrations in the system. *Journal of Hydraulic Research*, Vol. 18, pp. 59-82, 1980.
- [12] Taylor, G.W., Burns, J.R., Kammann, S.M., Powers, W.B. and Welsh, T.R. The energy harvesting Eel: A small subsurface ocean/river power generator. *IEEE Journal of Oceanic Engineering*, Vol. 26, No. 4, pp. 539-547, 2001.
- [13] Pobering, S. and Schwesinger, N. A novel hydropower harvesting device. *International Conference on MEMS, NANO and Smart Systems, ICMENS*, Banff, Alberta, Canada, pp. 480-485, August 25 - August 27, 2004.
- [14] Dickson, R.M. *New Concepts in Renewable Energy*, Lulu Enterprises Inc., 2008.
- [15] Li, S. and Lipson, H. Vertical-stalk flapping-leaf generator for wind energy harvesting, *ASME Conference on Smart Materials, Adaptive Structures and Intelligent Systems, SMASIS2009*, Oxnard, California, USA, September 21 - September 23, pp. 611-619, 2009.
- [16] Bryant, M., Mahtani, R. and Garcia, E. Synergistic Wake Interactions in Aeroelastic Flutter Vibration Energy Harvester Arrays. *ASME Conference on Smart Materials, Adaptive Structures and Intelligent Systems, SMASIS*, Scottsdale, Arizona, USA, September 18 - September 21, pp. 1-7, 2011.
- [17] Bryant, M., Mahtani, R. and Garcia, E. Wake synergies enhance performance in aeroelastic vibration energy harvesting. *Journal of Intelligent Materials Systems and Structures (JIMSS)*, Vol. 23, No. 10, pp. 1131-1141, 2012.
- [18] Deivasigamani, A., McCarthy, J.M., Watkins, S., John, S.J. and Coman, F. Flow induced flutter of slender cantilever high-compliance plates. *28th International Congress Of The Aeronautical Sciences, ICAS 2012*, September 23 - September 28, Brisbane, Australia, 2012.
- [19] McCarthy, J.M., Deivasigamani, A., John, S.J. Watkins, S. and Coman, F. The effect of the configuration of the amplification device on the power output of a piezoelectric strip. *ASME Conference on Smart Materials, Adaptive Structures and Intelligent Systems, SMASIS2012*, September 19 - September 21, Stone Mountain, Georgia, USA, 2012.
- [20] Deivasigamani A, McCarthy J.M, John S, Watkins S, Trivailo P, Coman F. Flutter of Cantilevered Interconnected Beams with Variable Hinge Position, *Journal of Fluids and Structures*, 38, pp. 223-237, 2013.
- [21] McCarthy, J.M., Deivasigamani, A., John, S.J., Watkins, S. and Coman, F., Peterson P. Downstream Flow Structures Of A Fluttering Piezoelectric Energy Harvester, *Journal of Experimental Thermal and Fluid Science*, Vol. 51, pp.279-290, 2013.

Contact Author Email Address

arvind.deivasigamani@student.rmit.edu.au

Copyright Statement

The authors confirm that they, and/or their company or organization, hold copyright on all of the original material included in this paper. The authors also confirm that they have obtained permission, from the copyright holder of any third party material included in this paper, to publish it as part of their paper. The authors confirm that they give permission, or have obtained permission from the copyright holder of this paper, for the publication and distribution of this paper as part of the ICAS 2014 proceedings or as individual off-prints from the proceedings.